Inorg. Chem. **2007**, *46*, 3295–3300

Stabilization of Acepentalene by Coordination to Transition Metals: A DFT Investigation

Andrés Vega[†] **and Jean-Yves Saillard***[,‡]

Departamento de Quimica, Facultad de Ecología y Recursos Naturales, Universidad Nacional Andres Bello, Republica 275, Santiago, Chile, and Sciences Chimiques de Rennes, UMR-CNRS 6226, Université de Rennes 1, 35042 Rennes Cedex, France

Received January 17, 2007

The possibility of stabilizing the unstable acepentalene (acp) molecule through coordination to transition metals is investigated by means of DFT calculations. Comparison with related experimentally known pentalene complexes indicate that their acp homologues are just slightly less stable, suggesting that they could be synthesized and isolated. Other original mono- and trinuclear species, such as $M(acp)_2$ (M = Zr, Hf), $Co_3(acp)_2^-$, and $Nb_3(acp)_2^+$, are also predicted to be stable.

Introduction

Pentalene (C_8H_6) and acepentalene ($C_{10}H_8$) are rather unstable antiaromatic molecules which have attracted much attention both from the theoretical and synthetic points of view.[1] Their aromatic dianions (Scheme 1) have been isolated as lithium salts, and their X-ray molecular structure are known.[1] A highly attractive way to stabilize pentalene is to complex it to transition metals. Indeed, complexes of pentalene[2,3] have been known for a very long time, and their rich structural chemistry presents a wide variety of coordination modes in which pentalene can bind to one, two, or three metal centers with a coordination mode varying from η^8 to η^3.[2] We recently undertook a theoretical investigation of the structure and stability of pentalene transition metal complexes, including hypothetical species which are predicted to be sufficiently stable to be isolated.[4]

Scheme 1. 10-π-Electron Pentalene Dianion and the 12-π-Electron Acepentalene Dianion

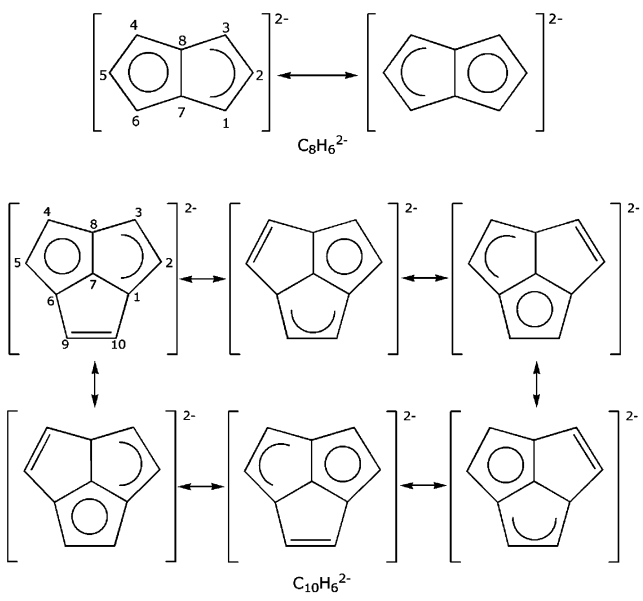

Surprisingly, unlike pentalene, a very small number of transition metal complexes of acepentalene have been reported so far,[1b] and more importantly no crystal structure has been determined. The existence of $(CO)_3Fe(acp)$ (acp = acepentalene) was suggested some time ago.[5] A few years later, the structures of $[Cp(CO)_2Fe]_2(acp)$, $Cp_2Zr(acp)$,

* To whom correspondence should be addressed. E-mail: saillard@univ-rennes1.fr. Fax: Fax: (+33) 2 23 23 68 40.
[†] Universidad Nacional Andres Bello.
[‡] Université de Rennes 1.

(1) (a) Zywietz, T. K.; Jiao, H.; Schleyer, P. v. R.; de Meijere, A. *J. Org. Chem.* **1998**, *63*, 3417−3422. (b) de Meijere, A.; Haag, R.; Schüngel, F.-M.; Kozhushkov, S. I.; Emme, I. *Pure Appl. Chem.* **1999**, *71*, 253−264.
(2) (a) Butenschön, H. *Angew. Chem., Int. Ed. Engl.* **1997**, *36*, 1695−1697. (b) Cloke, F. G. N. *Pure Appl. Chem.* **2001**, *73*, 233−238. (c) Summerscales, O. T.; Cloke, F. G. A. *Coord. Chem. Rev.* **2006**, *250*, 1122−1140.
(3) For selected complexes, see: (a) Katz, T. J.; Rosenberg, M. *J. Am. Chem. Soc.* **1963**, *85*, 2030−2031. (b) Bunel, E. E.; Valle, L.; Jones, N. L.; Carroll, P. J.; Barra, C.; González, M.; Muñoz, N.; Visconti, G.; Aizman, A.; Manríquez, J. M. *J. Am. Chem. Soc.* **1988**, *410*, 6596−6598. (c) Jonas, K.; Gabor, B.; Mynott, R.; Angermund, K.; Heinemann, O.; Krüger, C. *Angew. Chem., Int. Ed. Engl.* **1997**, *36*, 1712−1714. (d) Jonas, K.; Kolb, P.; Kollbach, G.; Gabor, B.; Mynott, R.; Angermund, K.; Heinemann,. O.; Kruger, C. *Angew. Chem., Int. Ed. Engl.* **1997**, *36*,1714−1718. (e) Cloke, F. G. N.; Green, J. C.; Jardine, C. N.; Kuchta, M. C. *Organometallics* **1999**, *18*, 1087−1090. (f) Jones, S. C.; O'Hare, D. *J. Chem. Soc., Chem. Comm.* **2003**, 2208−2209.
(4) Bendjaballah, S.; Kahlal, S.; Costuas, K.; Bévillon, E.; Saillard, J.-Y. *Chem. Eur. J.* **2006**, *12*, 2048−2065.

10.1021/ic070083l CCC: $37.00
Published on Web 03/09/2007

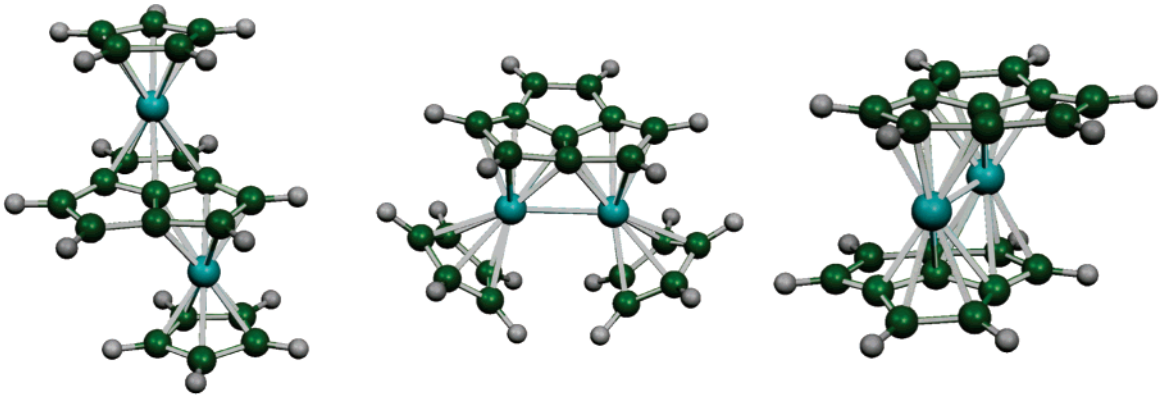

Figure 1. DFT-optimized structures of *anti*-(CpFe)$_2$(η^5,η^5-acp), *syn*-(CpV)$_2$(η^5,η^5-acp), and *syn*-Mo$_2$(η^5,η^5-acp)$_2$.

Table 1. DFT Computed Data for *anti*-[(FeCp)$_2$(acp)], *anti*-[(FeCp)$_2$(pent)], *syn*-[(VCp)$_2$(acp)], *syn*-[(Vcp)$_2$(pent)], Mo$_2$(acp)$_2$, and Mo$_2$(pent)$_2$[a]

	anti-[(FeCp)$_2$(acp)] C_2[b] $S=0$	*anti*-[(FeCp)$_2$(pent)] C_{2h}[c] $S=0$	*syn*-[(VCp)$_2$(acp)] C_s[b] $S=1$	*syn*-[(Vcp)$_2$(pent)] C_{2v}[c] $S=1$	[Mo$_2$(acp)$_2$] C_{2h}[b] $S=0$	[Mo$_2$ (pent)$_2$] D_{2h}[c] $S=0$
M−C1	2.201	2.165 [2.120]	2.313	2.244 [2.221]	2.485	2.423 [2.396]
M−C2	2.048	2.062 [2.025]	2.236	2.281 [2.236]	2.325	2.295 [2.281]
M−C3	2.047	2.051 [2.016]	2.316		2.331	2.294 [2.259]
M−C4	2.129					
M−C5	2.136					
M−C7			2.179	2.310 [2.305]	2.326	
M−C8			2.327		2.373	
M−C(pent-acp) (av)	2.112	2.085	2.274	2.272 [2.245]	2.368	2.327
M−C(Cp) (av)	2.086	2.089 [2.068]	2.335	2.340 [2.276]		
M−M	4.093		2.536	2.514 [2.538]	2.363	2.370 [2.340]
∑CCC at C$_7$[f]	360		354		359	
HOMO−LUMO gap (eV)	1.20	1.34			0.76	0.70
bonding energy between fragments (eV)	−25.28[b,d]	−26.56[c,d]			−68.48[b,e]	−69.56[c,e]

[a] Experimental x-ray data of pentalene complexes are given in parenthesis. Distances and angles are in Å and deg, respectively. [b] This work. [c] Ref 4. [d] One (FeCp)$_2^{2+}$ and one acp^{2-} or pent^{2-} fragment. [e] Two Mo^{2+} and two acp^{2-} or pent^{2-} fragments. [f] Sum of the bond angles around the central carbon atom.

Cp$_2$Hf(acp), and U(acp)$_2$ were proposed on the basis of NMR data.[1b] In this paper, we report a density functional theory (DFT) investigation on hypothetical complexes of acepentalene, some of them being isoelectronic to stable X-ray-characterized complexes of pentalene. The results are compared with a series of similar calculations carried out recently in our group on transition metal complexes of pentalene.[4]

Results and Discussion

Hypothetical Acepentalene Analogues of Isolated Pentalene Complexes. We start with the acepentalene analogues of the structurally characterized *anti*-[(C$_5$Me$_5$)Fe)$_2$(η^5,η^5-pent),[3b] *syn*-(CpV)$_2$(η^5,η^5-pent)[3f] (pent = pentalene), and Mo$_2$[η^5,η^5-C$_8$H$_4$(1,4-SiPr$^i_3$)$_2$]$_2$,[3e] that is, *anti*-(CpFe)$_2$(η^5,η^5-acp), *syn*-(CpV)$_2$(η^5,η^5-acp), and Mo$_2$(η^5,η^5-acp)$_2$. The ground-state optimized geometries are shown in Figure 1, and selected computed data are given in Table 1, together with those we previously obtained at the identical computational level for *anti*-(CpFe)$_2$(η^5,η^5-pent), *syn*-(CpV)$_2$(η^5,η^5-pent), and *syn*-Mo$_2$(η^5,η^5-pent)$_2$.[4]

Anti-(CpFe)$_2$(η^5,η^5-pent) is the archetype model for a series of diamagnetic 34-electron complexes of general formula (ML$_3$)$_2$(η^5,η^5-pent),[3b,6] for which we have provided a rationalization of the peculiar stability and absence of the metal−metal bond.[4] Its acepentalene counterpart, *anti*-(CpFe)$_2$(η^5,η^5-acp), exhibits a similar geometry and electronic sructure. Its Fe−C distances are on average slightly longer than those of its pentalene relative. The HOMO−LUMO gap is slightly smaller but is still large. The computed bonding energy between acp^{2-} and two CpFe$^+$ units is 5% lower than that between pent^{2-} and two CpFe$^+$ units in the pentalene homologue. Clearly, the stabilities of (CpFe)$_2$(acp) and (CpFe)$_2$(pent) are comparable.

The 28-electron complex *syn*-(CpV)$_2$(η^5,η^5-pent) is antiferromagnetic and exhibits a V−V bond distance of 2.54 Å,[3f] which we have described as a weak bond with a formal order of 2.5.[4] The computed electronic structures of *syn*-(CpV)$_2$(η^5,η^5-pent) and *syn*-(CpV)$_2$(η^5,η^5-acp) exhibit similar characteristics. The optimized V−C distances of *syn*-(CpV)$_2$-(η^5,η^5-acp) are on average very close to those obtained for its pentalene relative, with a slightly longer V−V optimized distance. Both complexes are computed to have a triplet ground state lying not far below the singlet state (0.31 and

(5) Butenschön, H.; De Meijere, A. *Angew. Chem., Int. Ed. Engl.* **1984**, 707−708.

(6) (a) Manríquez, J. M.; Ward, M. D.; Reiff, W. M.; Calabrese, J. C.; Jones, N. L.; Carroll, P. J.; Bunel, E. E.; Miller, J. S. *J. Am. Chem. Soc.* **1995**, *117*, 6182−6193. (b) Jones, S. C.; Hascall, T.; Barlow, S.; O'Hare, D. *J. Am. Chem. Soc.* **2002**, *124*, 11610−11611.

Table 2. DFT Computed Data for $(CO)_3Fe(\eta^{5/3}\text{-acp})$, $(CO)_3Fe(\eta^{5/3}\text{-pent})$, $CpFe(\eta^5\text{-acp})^+$, and $CpFe(\eta^5\text{-pent})^+$[a]

	$[(CO)_3Fe(\eta^{5/3}\text{-acp})]$ C_s[b] $S=0$	$[(CO)_3Fe(\eta^{5/3}\text{-pent})]$ C_s[c] $S=0$	$[CpFe(\eta^{5/3}\text{-acp})]^+$ C_s[b] $S=0$	$[CpFe(\eta^{5/3}\text{-acp})]^+$ C_s[c] $S=0$
M−C4	2.133	2.165	2.104	2.111
M−C5	2.133		2.104	
M−C6	2.353		2.144	
M−C7	2.125	2.059	2.001	2.084
M−C8	2.353	2.428	2.144	2.101
M−C(acp/pent) (av)	2.219	2.236	2.099	2.096
M−C(Cp/CO) (av)			2.137	2.130
∑CCC at C_7			356.0	
HOMO−LUMO gap (eV)	1.33	1.51	0.496	0.68

[a] Distances and angles are in Å and deg, respectively. [b] This work. [c] Ref 4.

0.36 eV for the pentalene[4] and acepentalene derivatives, respectively). In both complexes, the singlet state corresponds to a weak V−V triple bond made of one δ and two π bonds.[4] In the triplet ground state, the V−V δ^* MO is singly occupied so that the very weak V−V δ bond is half cancelled. The computed bonding energies between the dianionic ligands and two CpV^+ units (3 fragments) are on the same order of magnitude in both compounds.

$Mo_2(\eta^5,\eta^5\text{-acp})_2$ is found to be a singlet ground state with an electronic structure similar to that found for $Mo_2(pent)_2$, that is, with a formal Mo−Mo bond order between 2 and 3.[4] It adopts the anti (C_{2h}) conformation of the acp ligands. Again, the metric and energetic data computed for the acepentalene and pentalene homologues are quite similar, suggesting similar stabilities. In particular, the bonding energy between two Mo^{4+} and two dianionic ligands (4 fragments) was found to be only 2% lower in the acp derivative. The triplet state was found to be less stable than the singlet state by 0.45[4] and 0.62 eV for the pentalene and acepentalene derivatives, respectively.

Thus, DFT calculations (bond lengths, bonding energies, and vibrational frequencies) indicate that the thermodynamic stabilities of *anti*-$(CpFe)_2(\eta^5,\eta^5\text{-acp})$, *syn*-$(CpV)_2(\eta^5,\eta^5\text{-acp})$, and $Mo_2(\eta^5,\eta^5\text{-acp})_2$ are comparable to those of their pentalene homologues. With the major characteristics of the electronic structures also being similar, one may also expect comparable chemical stabilities. However, the presence of a free formal double bond on the uncoordinated ring in the acp complexes (see Scheme 1) raises the question of their reactivity with respect to a [2 + 2] dimerization. The significant HOMO−LUMO gaps computed for these complexes (similar to those of their pentalene counterparts) suggest moderate (if any) reactivity. This is also supported by the computed distances of the uncoordinated C=C bond (1.398, 1.397, and 1.396 Å for the Fe, V, and Mo species, respectively), which are indicative of significant π delocalization over the ring.

Other Mononuclear Acepentalene Complexes. Assuming, from the above results, that some acepentalene complexes should be stable enough to be isolated, we have investigated the stability and structure of other acepentalene complexes for which no simple pentalene analogue has been characterized. We start with the mononuclear $(CO)_3Fe(acp)$ (acp = acepentalene) species, the existence of which was suggested some time ago.[5] For the models described above,

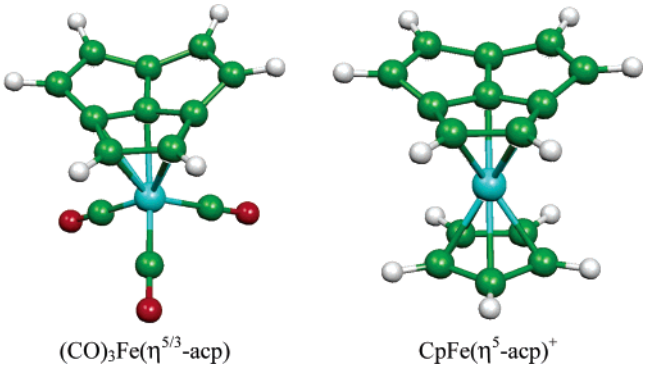

Figure 2. DFT-optimized structures of $(CO)_3Fe(\eta^{5/3}\text{-acp})$ and $CpFe(\eta^5\text{-acp})^+$.

our results are compared with those obtained previously for the pentalene derivative.[4] Selected computed data are given in Table 2, and the optimized structure is shown in Figure 2. Again, the computed data obtained for both pentalene and acepentalene derivatives are rather similar. Both compounds exhibit similar electronic, energetic, and structural features, with an $\eta^{5/3}$ coordination mode, that is, intermediate between η^5 (18-electron ML_6 type) and η^3 (16-electron ML_5 type).[4] Calculations on the isoelectronic $(CO)_3Co(acp)^+$ and $CpFe(acp)^-$ models yielded similar results (see Supporting Information). With two less electrons, the $CpFe(acp)^+$ model was also investigated and compared to the $CpFe(pent)^+$ model[4] (Table 2 and Figure 2), to which a structurally characterized derivative exhibiting a substituted pentalene ligand, namely, $CpFe(\eta^5\text{-}C_8H_4Fc_2)^+$ (Fc = ferrocenyl), corresponds.[7] Both model compounds are electron deficient, with the electron deficiency delocalized on both the metal and the non-coordinated rings of the ligand, suggesting that donor-substituted acepentalene complexes of 12-electron ML_n moieties such as $CpFe^+$ should be isolable.

When ML_n moieties of electron counts lower than 12 were considered in the calculations, no stable $(ML_n)(acp)$ diamagnetic structure could be found, unlike in the pentalene series where the η^8 coordination permits the conjugated ligand to donate all its π electrons to the metal, allowing it to reach (or to approach) the 18-electron count, such as in $CpV(\eta^8\text{-pent})$ or $M(\eta^8\text{-pent})_2$ (M = Ti, Zr).[3c,d,4] Indeed, the η^8 coordination of pentalene requires it to fold around its central

(7) Lukasser, J.; Angleitner, H.; Schottenberger, H.; Kopacka, H.; Schweiger, M.; Bildstein, B.; Ongania, K.-H.; Wurst, K. *Organometallics* **1995**, *14*, 5566−5578.

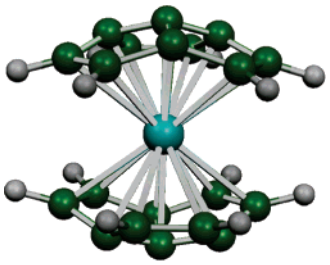

Figure 3. Optimized structure of Zr(η^{10}-acp)$_2$. The computed structure for Hf(η^{10}-acp)$_2$ is very similar.

Table 3. DFT Computed Data for Zr(η^{10}-acp)$_2$, Zr(η^8-pent)$_2$, and Hf(η^{10}-acp)$_2$[a]

	Zr(η^{10}-acp)$_2$ D_{3d}[b] $S = 0$	Zr(η^8-pent)$_2$ D_2[c] $S = 0$	Hf(η^8-acp)$_2$ D_{3d}[b] $S = 0$
M−C1	2.477	2.353	2.477
M−C2	2.668	2.601	2.668
M−C3		2.731	
M−C4		2.559	
M−C7	2.405		2.405
M−C(acp) (av)	2.584	2.561	2.584
∑CCC at C$_7$[e]	343		343
HOMO−LUMO gap (eV)	2.69	2.58	2.69
bonding energy between fragments (eV)	−92.45[b,d]	−95.85[c,d]	−103.61

[a] Distances and angles are in Å and deg, respectively. [b] This work. [c] Ref 4. [d] One Zr^{4+} and two acp^{2-} or $pent^{2-}$ fragments. [e] Sum of the bond angles around the central carbon atom.

C−C bond, forcing its C_5 rings to make an angle of ∼130−150°.[1,4] In the case of the investigated hypothetical (ML$_n$)-(acp) models, such a distortion was found to not be possible because of the rigidity imposed by the existence of a third C_5 ring. As a consequence, these species cannot be stable. On the other hand, the bis-acepentalene d^0 M(η^{10}-acp)$_2$ (M = Zr, Hf) complexes were found to be energy minima (Figure 3 and Table 3). These sandwich species adopt a staggered conformation of the acp ligands (D_{3d} symmetry), the eclipsed conformation (D_{3h}) being 0.23 and 0.24 eV less stable for M = Zr and Hf, respectively. They can be described as 18-electron complexes. Indeed, the d^0 M(IV) center is bonded to two 12-electron donor acp^{2-} which can each donate only 9 electrons on average to the metal by symmetry. This situation is sketched in Figure 4. The 9 metal AO's match the $2 \times a_{1g} + a_{2u} + 2 \times e_g + e_u$ symmetries, whereas the occupied π combinations of both acp^{2-} ligands match the $2 \times a_{1g} + 2 \times a_{2u} + 2 \times e_g + 2 \times e_u$ symmetries. As a result, one a_{2u} and one e_u ligand combinations remain nonbonding with respect to the metal, and the 6 electrons they contain are not part of the metal environment. This situation is related to that of the M(pent)$_2$ (M = d^0) complexes which are apparent 20-electron complexes but, effectively, are 18-electron complexes.[4] The DFT-computed MO diagram of Zr(acp)$_2$ shown in Figure 5 is fully consistent with the simplified scheme of Figure 4. The three highest-occupied MOs have negligible metal character. The LUMO of the complex derives from the LUMO of free acp^{2-} and has no metal participation by symmetry. The η^{10} coordination is attained through some "umbrella-type" distortion away from planarity of the acp ligands. The dihedral angle between

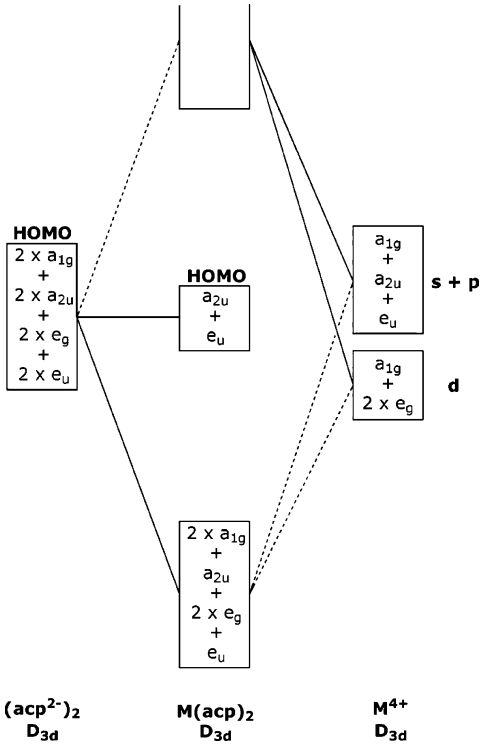

Figure 4. Simplified MO diagram for a d^0 M(η^{10}-acp)$_2$ complex.

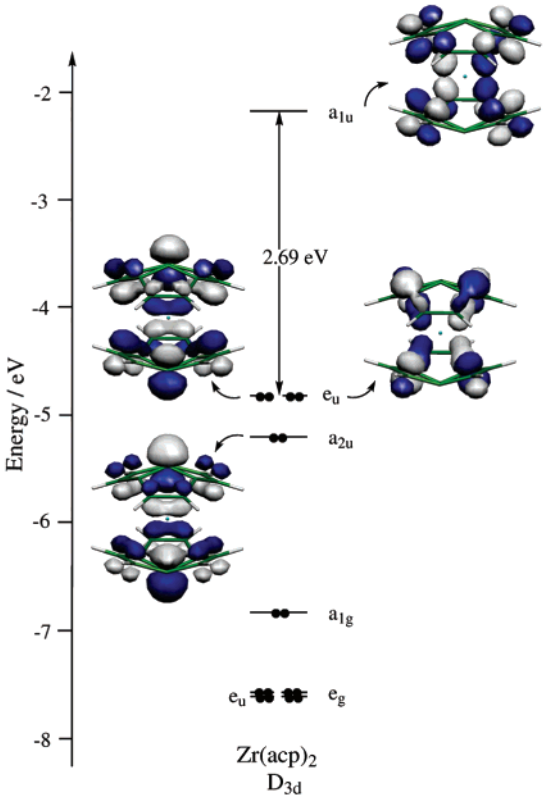

Figure 5. Computed MO diagram of Zr(acp)$_2$.

two adjacent C_5 rings is 145° for both the Zr and Hf complexes. In this η^{10} coordination mode, the carbon atoms do not similarly interact with the metal, the six outer ones being weakly bonded so that if these interactions are neglected the bonding mode can be somewhat approximated to that of trimethylenemethane complexes. Nevertheless, the

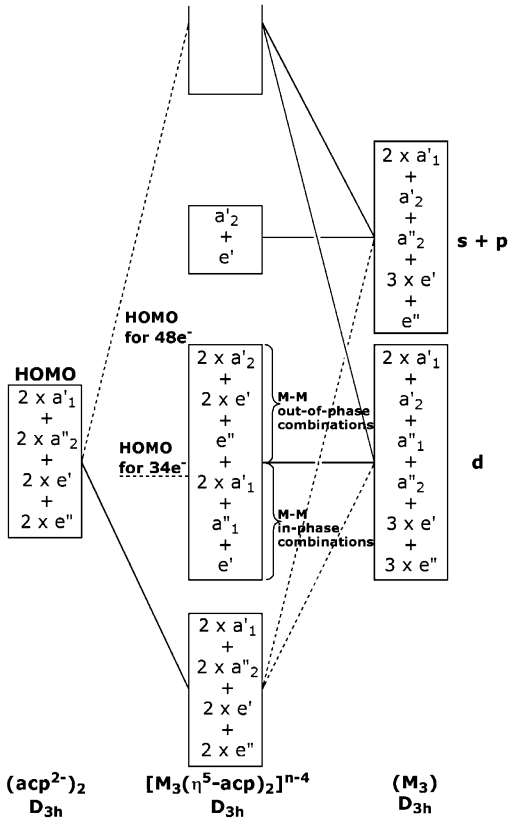

Figure 6. Simplified MO diagrams for diamagnetic 48- and 34-electron $M_3(\eta^5, \eta^5,\eta^5\text{-acp})_2$ complexes.

average Zr−C distance in $Zr(\eta^{10}\text{-acp})_2$ (2.547 Å) compares well with the corresponding value obtained for $Zr(pent)_2$ (2.561 Å),[4] as well as the bonding energy between Zr^{4+} and two dianionic ligands, which is only 4% lower in the acp derivative. The significant value of the computed HOMO−LUMO gaps supports the stability of such diamagnetic species. It is noteworthy that these hypothetical compounds are isoelectronic with $U(acp)_2$ which has been claimed to exist and for which a similar sandwich structure has been suggested an the basis of NMR experiments.[1b]

Hypothetical Trinuclear Bisacepentalene Complexes. The existence of three equivalent rings on acepentalene raises the possibility for trinuclear systems. Our search for stable bisacepentalene trinuclear sandwich complexes ended up with two favorable closed-shell electron counts, 48- and 34-electrons, both of D_{3h} symmetry. These two situations are sketched in the simplified MO diagram of Figure 6.

The former corresponds to the $[Co_3(acp)_2]^-$ model for which the optimized geometry is shown in Figure 7, and the major computed data are given in Table 4. In this compound, the 12 occupied ligand π-type combinations can interact by symmetry with only 9 of the 12 metal 4s/4p vacant combinations, which are the major electron-accepting metal AOs (see Figure 6). Thus, 3 additional metal combinations, of a''_1 and e'' symmetry, have to be provided by the 3d block for interaction with the ligands. As a result, the 12 (among the 15) low-lying 3d-type combinations which are not involved in the bonding with the ligands are occupied. On the other hand, there are three 4s/4p Co−Co combinations (a'_2 and e') which cannot interact by symmetry with the ligand orbitals. They are left vacant because of their high energy. This simple symmetry-based picture is sufficient to rationalize the closed-shell situation of the 48-electron $[Co_3(acp)_2]^+$ model (Figure 6). One should take into account, however, that in the real situation important mixing between 4s/4p and 3d orbitals occurs, inducing significant Co−Co bonding, as exemplified by the corresponding distance of 2.605 Å (Table 4). Thus, we are in the classical stable closed-shell situation of a triangular 48-electron trinuclear species exhibiting three metal−metal single bonds. The question which then arises is which are the MOs of Figure 6 that are associated with the three Co−Co bonds. Group theory tells us that the three Co−Co bonding occupied MOs are of a'_1 and e' symmetry, whereas the three antibonding vacant ones are of e' and a'_2 symmetry. The latter are easily identified as the 4s/4p e' and a'_2 combinations which are metal−ligand nonbonding but strongly metal−metal antibonding. The a'_1 and e' bonding counterparts are part of the 12 3d-type combinations which are not involved in the bonding with the ligands. Exploration of the DFT results indicates that the Co−Co bonding character of these levels is the result of significant mixing of the 4s/4p obitals into the 3d block. This mixing prevents also the M−M out-of-phase combinations to exhibit significant antibonding character, at least in the M = Co case. Finally, one should note that, with a rather long Co−C_7 distance, the η^5 coordination mode of the metal centers in this model is significantly distorted toward η^3.

The η^5 coordination is more symmetrical in the optimized $[Nb_3(acp)_2]^-$ model which exemplifies the case of 34-electron closed-shell species. This situation is obtained by depopulat-

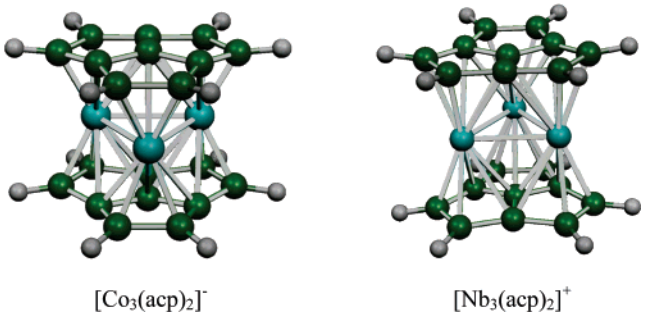

Figure 7. Optimized structures of $[Co_3(acp)_2]^-$ and $[Nb_3(acp)_2]^+$.

Table 4. DFT Computed Data $[Co_3(acp)_2]^-$ and $[Nb_3(acp)_2]^{+a}$

	$[Co_3(acp)_2]^-$ $D_{3d}{}^b$ $S = 0$	$[Nb_3(acp)_2]^+$ $D_{3d}{}^b$ $S = 0$
M−C1	2.354	2.581
M−C2	2.014	2.383
M−C7	2.443	2.567
M−C(acp) (av)	2.159	2.470
M−M	2.605	2.622
∑CCC at C_7	359.1	359.6
HOMO−LUMO gap (eV)	1.34	1.02
bonding energy between fragments (eV)	−62.60[c]	−103.17[c,d]

[a] Distances and angles are in Å and deg, respectively. [b] This work. [c] One $(Co_3)^{3+}$ and two $(acp)^{2-}$ fragments. [d] One $(Nb_3)^{3+}$ and two $(acp)^{2-}$ fragments.

ing the seven M−M out-of-phase combinations in the d-block of the $M_3(acp)_2$ species (Figure 6), namely, σ^* (e′and a′$_2$), π^* (e″) and δ^* (e′). The 4d AOs of Nb are much more diffuse than the 3d AOs of Co. As a result, in the case of Nb, the d-type metal−metal out-of-phase combinations are significantly antibonding. Similarly, their in-phase counterparts, σ (a′$_1$ and e′, π (a″$_1$) and δ (a′$_1$), are significantly Nb−Nb bonding. With five bonding electron pairs, one is left with an M−M bond order of 1.67. The computed HOMO−LUMO gap and Nb−C bond distances (Figure 6 and Table 4) suggest significant stability for such a species. It is likely that $M_3(acp)_2$ open-shell (or perhaps closed-shell) species with electron counts between 48 and 34 (or even lower than 34) should also be attainable.

Computational Details

DFT[8] calculations were carried out using the ADF package[9] at the identical level of theory as those of Bendjaballah et al.,[4] that is, with the local VWN parametrization,[10] the nonlocal BP86 corrections,[11,12] and the use of the standard TZP atomic basis sets. The frozen core approximation was used to treat core electrons[8d] at the following level: C, O 1s; Fe, V, Co, Mn 3p; Mo, Zr, Nb 3d; and Hf, 4d. Full geometry optimizations were carried out on each complex using the analytical gradient method implemented by Verluis and Ziegler.[13] Spin-unrestricted calculations were performed for the open-shell systems. Optimized geometries have been characterized as energy minima by calculations of their normal vibrational modes (imaginary frequencies lower than 54*i* cm^{-1} and associated with rotation of Cp ligands were neglected). Fragment interaction analysis was done using the method proposed by Ziegler.[14] Molecular and orbital plots were done with MOLEKEL 4.3,[15] and the other graphic materials were produced with CHEMDRAW8.0.[16]

Conclusion

The comparison of the electronic and geometric structures of hypothetical acepentalene complexes with isoelectronic experimentally characterized complexes of pentalene, suggests that the former series should be only slightly less stable than the latter. These results and those obtained in the exploration of the original coordination modes support early reports[1b] in the prediction that the stabilization of acepentalene is possible through its complexation (formally as acp^{2-}) to one, two, or three transition metals, in the same way that stabilization of pentalene through metal complexation has been shown to exist.[2,3] We predict that, as soon as synthetic routes or isolation techniques are found, acepentalene complexes will be structurally characterized in the solid state.

Acknowledgment. This work was supported by the Franco/Chilean grant CNRS/CONICYT 18176 and by the Chilean grants FONDECYT 11060176 and DI-UNAB 20-06/R. Calculations were carried out at the French national computing centers IDRIS (Orsay, France) and CINES (Montpellier, France).

Supporting Information Available: Cartesian coordinates for all the optimized structures. This material is available free of charge via the Internet at http://pubs.acs.org.

IC070083L

(8) (a) Baerends, E. J.; Ellis, D. E.; Ros, P. *Chem. Phys.* **1973**, *2*, 41. (b) Baerends, E. J.; Ross P. *Int. J. Quantum Chem.* **1978**, *S12*, 169. (c) Boerrigter, P. M.; te Velde, G.; Baerends E. *J. Int. J. Quantum Chem.* **1988**, *33*, 87. (d) te Velde, G.; Baerends E. *J. Comput. Phys.* **1992**, *99*, 84.
(9) *Amsterdam Density Functional (ADF) Program*, version ADF2002.01; Vrije Universiteit: Amsterdam, The Netherlands, 2002.
(10) Vosko, S. D.; Wilk, L.; Nusair, M. *Can. J. Chem.* **1990**, *58*, 1200.
(11) (a) Becke, A. D. *J. Chem. Phys.* **1986**, *84*, 4524. (b) Becke, A. D. *Phys. Rev. A* **1988**, *38*, 2098.
(12) (a) Perdew, J. P. *Phys. Rev. B* **1986**, *33*, 8882. (b) Perdew, J. P. *Phys. Rev. A* **1986**, *34*, 7406.
(13) Verluis, L.; Ziegler, T. *J. Chem. Phys.* **1988**, *88*, 322.
(14) te Velde, G.; Bickelhaupt, F. M.; Fonseca Guerra, C.; van Gisbergen, S. J. A.; Baerends, E. J.; Snijders, J. G.; Ziegler, T. J. *J. Comput. Chem.* **2001**, *22*, 931.
(15) Flükiger, P.; Lüthi, H. P.; Portmann, S.; Weber, J. *MOLEKEL 4.3*; Swiss Center for Scientic Computing: Manno, Switzerland, 2000−2002.
(16) *ChemDraw 8.0*; CambridgeSoft Corporation: Cambridge, MA, 2003.